



Cite this: *Green Chem.*, 2025, **27**, 14317

## Rational catalyst design for acetaldehyde upgrading – an in-depth study on the use of a solid base and the development of a second generation supported N-heterocyclic carbene catalyst

Maurice Belleflamme, <sup>a,b</sup> Stefan Mersmann,<sup>a</sup> Ridvan Ince,<sup>b</sup> Thomas Wiegand, <sup>a,b</sup> Walter Leitner <sup>a,b</sup> and Andreas J. Vorholt <sup>\*a</sup>

Herein, we report the development of a second-generation supported N-heterocyclic carbene (NHC) catalyst to significantly improve the upgrading of acetaldehyde to 3-hydroxy-2-butanone (acetoin) and suppress catalyst deactivation *via* leaching, aided by the use of sodium carbonate ( $\text{Na}_2\text{CO}_3$ ) as a solid base. We were able to demonstrate that the activity of the catalyst benefits from the use of finer sieve fractions of solid  $\text{Na}_2\text{CO}_3$ . In addition, we found a beneficial effect of intermittent addition of  $\text{Na}_2\text{CO}_3$  on the productivity of an earlier reported supported NHC catalyst over a total duration of 10 h time-on-stream (TOS). Despite the addition of the solid base, excellent selectivity towards acetoin,  $S(\text{acetoin}) > 90\%$ , was found throughout batch and continuous flow experiments. Unfortunately, deactivation of the catalyst could not be suppressed by using excess base. Therefore, a second-generation supported NHC catalyst was developed, bearing non-nucleophilic counterions to suppress the reverse Menshutkin decomposition pathway. The developed catalyst was found to be active for more than 60 h TOS, attaining very high selectivities towards acetoin,  $S(\text{acetoin}) > 88\%$ , and single-pass conversion of acetaldehyde, losing only around 20% of catalytically active species through decomposition.

Received 15th July 2025,  
Accepted 22nd September 2025

DOI: 10.1039/d5gc03630e

[rsc.li/greenchem](https://rsc.li/greenchem)

### Green foundation

1. This work focuses on a stable, metal-free, heterogeneous organocatalyst for upgrading bio-based acetaldehyde into acetoin, improving efficiency for sustainable acetoin production in a 100% atom-efficient reaction, and paving the way for future research with regard to the use of acetoin as a bio-based platform chemical in a sustainable chemical value chain.
2. The productivity of our chemocatalyst with a space-time yield (STY) of  $19 \text{ g L}^{-1} \text{ h}^{-1}$  exceeds the STY of enzymatic processes by tenfold. Furthermore, experiments were carried out in green solvents under benign conditions.
3. Though exceptionally stable, the developed catalyst still bears a non-nucleophilic  $\text{PF}_6^-$  anion which could be replaced with other, non-fluorine-based anions to avoid the use of “forever chemicals”. Research regarding an even more stable third-generation catalyst, omitting the use of PFAS and further decreasing leaching behaviour, is currently ongoing in our laboratories.

## Introduction

In order to facilitate sustainable synthesis routes for various chemicals and fuels, upgrading of bio-mass derived ethanol has received a lot of attention recently. In particular, there is great interest in upgrading ethanol to bio-fuels to produce

middle-distillate fuels like jet and diesel fuels.<sup>1,2</sup> Besides extensive research on the use of ethanol as a drop-in fuel and feedstock for manufacturing hydrocarbon fuels, ethanol is also considered a building block for (bulk) chemicals like 1-butanol, acetone, acetic acid and 1,3-butadiene.<sup>3</sup> Upgrading ethanol generally starts with the dehydrogenation to acetaldehyde, followed by Guerbet or aldol reaction pathways.<sup>3-7</sup> Despite the use of optimal homogeneous catalysts, Guerbet reactions struggle with low conversions, while heterogeneous processes require harsh conditions and yield low selectivity. Ethanol is not ideal for these reactions due to the unfavourable

<sup>a</sup>Max Planck Institute for Chemical Energy Conversion, Stiftstraße 34-36, 45470

Mülheim an der Ruhr, Germany. E-mail: andreas-j.vorholt@cec.mpg.de

<sup>b</sup>Institute for Technical and Macromolecular Chemistry, RWTH Aachen University, Worringerweg 2, 52074 Aachen, Germany



dehydrogenation step and the challenging selective aldol condensation reaction of acetaldehyde under those harsh conditions.<sup>3,7–13</sup>

N-Heterocyclic carbenes (NHCs) offer a more selective method for coupling aldehydes, but their use is mainly limited to aromatic or long-chain alkyl aldehydes.<sup>14–16</sup> The NHC-catalysed self-addition of acetaldehyde to form 3-hydroxy-2-butanone (acetoin) is barely exploited in the literature, despite being crucial for upgrading bio-ethanol to C<sub>4</sub> chemicals like butenes and 2,3-butanediol. Although some NHC-based catalysts show promise, their stability and efficiency need to be improved before large-scale use.<sup>17,18</sup> For example, Zhang *et al.* reported that homogeneous thiazolium salts used in combination with solid bases can only be used for up to three cycles.<sup>18</sup> Along the recycling pathway, yields towards desired acetoin decreased from 98% to 55%. On the other hand, thiazolium salts immobilized on polystyrene as support materials, in combination with K<sub>2</sub>CO<sub>3</sub>, did not lead to satisfactory results (95% acetoin yield in the first run and <10% in the second run).<sup>17</sup>

In order to further investigate the applicability of NHC-catalysed upgrading of acetaldehyde to acetoin, a heterogeneous NHC catalyst was recently developed. The catalyst was prepared *via* grafting the catalytically active precursor molecule onto Merrifield's polymer resin.<sup>19</sup> In the homo-acyloin reaction of acetaldehyde to acetoin in ethanol as a solvent, a mild solid base (Na<sub>2</sub>CO<sub>3</sub>) was used to activate the catalyst *in situ*. Furthermore, although the base persisted in the system, very high selectivity towards the desired acetoin was observed.<sup>19</sup> The catalyst was found to be suitable for recycling as well as continuous flow applications, attaining a total turn-over-number (TON) of 111 after 10 h time-on-stream (TOS). Nuclear magnetic resonance (NMR) spectra in both solution and solid states showed that the apparent decay in catalytic activity with increasing TOS originates from the decomposition of the catalyst.<sup>19</sup> Strong evidence was found that the catalyst decomposes into its pristine building blocks according to the reverse Menshutkin reaction.<sup>20–23</sup> This reaction is commonly known for imidazolium-based halide salts.<sup>21</sup> In the heterogeneously catalysed acetaldehyde self-addition, about 39% of the catalytically active component was lost over a total of 10 h TOS.<sup>19</sup> In order to suppress the decomposition of the developed catalyst and attain a more productive catalytic system, two strategies will be further investigated. As the heterogeneous catalyst is activated by a solid base (Na<sub>2</sub>CO<sub>3</sub>), intermittent addition and/or co-feeding of the base have not been investigated yet and could provide valuable information about the mechanism of both activation and decomposition. Besides this, tackling the molecular decomposition pathway of the first-generation immobilised catalyst by applying catalyst design principles can result in further improvements as well (Scheme 1).

For example, Lemaire *et al.* investigated the influence of the nature of the anion as well as the bulkiness of the *N*-alkyl group in several thiazolium-based pre-catalysts for the retrobenzoin condensation of vegetable oil derivatives.<sup>23</sup> While

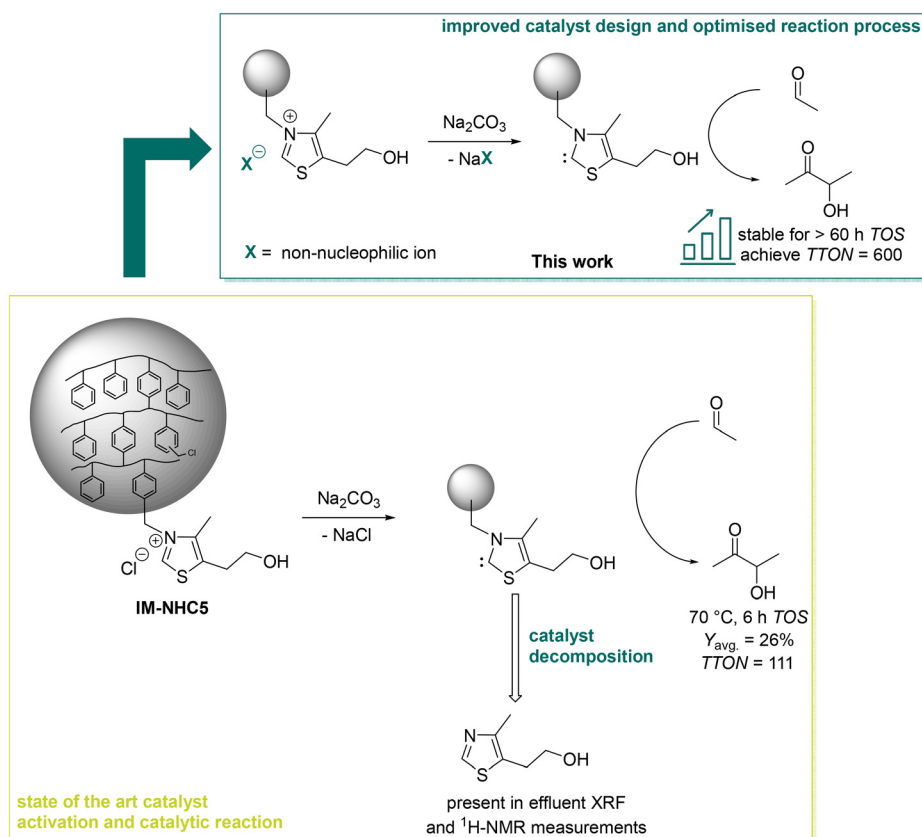
increasing the bulkiness of the alkyl side group resulted in a decrease in catalytic activity, different types of anions were not found to have a significant influence on the performance of the catalyst. However, when investigating the thermal stability of the thiazolium pre-catalysts with different anions, a substantial improvement in thermal stability was found when using larger anions like BF<sub>4</sub><sup>−</sup> and OTf<sup>−</sup> as opposed to simple halide anions like I<sup>−</sup> and Br<sup>−</sup>.<sup>23</sup> In this context, the hypothesis is that the stability of the developed heterogeneous catalyst and thus its tendency to undergo decomposition *via* the reverse Menshutkin reaction can be greatly improved by subjecting the developed **IM-NHC5** catalyst to an ion-exchange procedure with a non-nucleophilic and non-coordinating anion like PF<sub>6</sub><sup>−</sup>. Though the choice of this specific anion merely serves as a proof-of-concept for increased catalyst stability, combining this second-generation heterogeneous NHC catalyst with an in-depth study of the role of solid Na<sub>2</sub>CO<sub>3</sub> could result in a catalytic system that is much more stable in both batch recycling and continuous-flow experiments.

## Results and discussion

Motivated by the desire to improve the performance of the reported immobilised NHC catalyst system, we set out to investigate the effect of solid Na<sub>2</sub>CO<sub>3</sub> on the productivity of the system. In order to determine the degree of solubility of the Na<sub>2</sub>CO<sub>3</sub> in the reaction solution, X-ray fluorescence (XRF) measurements were performed on all postreaction samples. As the measured values for sodium in the postreaction samples were below detection limits, it can be concluded that Na<sub>2</sub>CO<sub>3</sub> remains solid throughout the reaction. Hence, based on these measurements, we assume that the activation of **IM-NHC5** has to proceed *via* a solid–solid interfacial surface reaction. However, the complete exclusion of any water from the reaction medium cannot be completely ruled out, as the solvent EtOH was used without further purification and drying. Nonetheless, the residual water in the used EtOH and the assumed minor solubility of Na<sub>2</sub>CO<sub>3</sub> therein are not assumed to have a significant effect on the activation of the immobilised catalyst. We envision that the amount of solid base and consequently the amount of solid base surface area present in the reaction vessel might have an influence as well (Table 1).

To demonstrate the importance of the presence of Na<sub>2</sub>CO<sub>3</sub> to yield the catalytically active species *via* a surface activation reaction, an experiment was conducted without any base (Table 1, entry 1.1). The acetoin yield is below the GC-FID detection limit. Instead, 1,1-diethoxyethane, 1-ethoxy-1-propoxyethane, and 1,1-dipropoxyethane were observed in the GC-FID measurements. This experiment highlights that it is not possible to generate the catalytically active species in the absence of base, as no acetoin is observed. On the other hand, using an under-stoichiometric amount of base (entry 1.2) results in a 40% acetoin yield as well as 21% by-products. The benchmark experiment, discussed in a recent publication, where a slight excess of base was used (entry 1.3), resulted in a 73% acetoin





**Scheme 1** Overview of the literature known **IM-NHC5**/ $Na_2CO_3$ -catalysed self-addition of acetaldehyde to acetoin (bottom) as well as the suggested improved catalytic system to achieve longer catalyst stability and time-on-stream using a modified version of the catalyst.<sup>19</sup> As a support material, a commercially obtained Merrifield's resin, DVB crosslinked, 16–50 mesh, 5.5 mmol  $g^{-1}$  Cl was used.

**Table 1** Results of the **IM-NHC5**-catalysed acetaldehyde self-addition in EtOH as the solvent using solid  $Na_2CO_3$  as the base<sup>a</sup>

Entry	$c(Na_2CO_3)$ (mol%)	Y (acetoin) <sup>b,c</sup> (%)	$\sum Y$ (side products) <sup>b,d</sup> (%)	TON (acetoin)
1.1	0 <sup>e</sup>	<0.1	38	—
1.2	1.3	40	21	22
1.3 <sup>f</sup>	2.6	73	5	36
1.4	5.2	82	4	40
1.5	10.4	83	3	40
1.6	26.0	83	4	42

<sup>a</sup> Reaction conditions: experiments were carried out using a stock solution containing acetaldehyde, ethanol and mesitylene in a 1:1:0.1 volumetric ratio.  $V(\text{stock}) = 2.0$  mL,  $n(\text{acetaldehyde}) \approx 19$  mmol,  $c(\text{IM-NHC5}) = 2$  mol%,  $T = 70$  °C,  $t = 2$  h, 1000 rpm. <sup>b</sup> As determined by GC-FID using mesitylene as the internal standard. <sup>c</sup> Acetoin yields including the yield of dimeric acetoin. <sup>d</sup> Side products include 1,1-diethoxyethane, paraldehyde and others. <sup>e</sup> In the absence of any base. <sup>f</sup> As seen and discussed in a recent publication.<sup>19</sup>

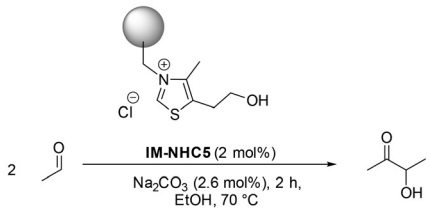
yield with a marginal amount of by-products (5%).<sup>19</sup> Comparison of these two experiments (entries 1.2 and 1.3) once more highlights that the activation of the catalyst proceeds *via* the solid base and that a lack of solid base in the system results in a decreased catalytic performance. The experiment shown in entry 1.4 indicates that doubling the amount of base to 5.2 mol% has a beneficial effect on the catalytic performance, as there is an increase in the observed acetoin yield from 73 to 82%. A possible explanation for the enhancing effect of the base on the catalytic performance of the system could be that the amount of base thus far used is not sufficient to activate the heterogeneous **IM-NHC5** catalyst. In the experiment shown in entry 1.4, the increased amount of base, and hence the increased available base surface, apparently activates a greater portion of the **IM-NHC5** pre-catalyst, also increasing the amount of product. However, further raising the base concentration to 10.4 mol% (entry 1.5) or even 26 mol% (entry 1.6) does not significantly improve the catalytic performance. Hence, the optimal ratio of catalyst to base is determined to be 1:5.2 based on the experiments shown in Table 1. Interestingly, increasing the amount of solid base does not influence the product spectrum of the reaction. The amounts of side products obtained are approximately the same in all experiments with a base concentration of



$\geq 2.6$  mol%. The experiments shown in Table 1 highlight that the amount of base present in the system plays a crucial role in the productivity of the system. At the same time, the product spectrum at higher base excess remains unaffected, and excellent selectivity towards acetoin is attained. As the amount of solid base plays such an important role in activating the solid catalyst, there will most certainly be a relationship between the particle size of the solid base and the effect on the catalytic productivity as well. Ideally, with finer base particles, a greater portion of the catalyst can be activated. To verify this, several experiments with defined particle sizes were carried out using different fine mesh sieves to strain the  $\text{Na}_2\text{CO}_3$  prior to use (Table 2). In addition, sieve fractions were dried and stored in an Ar-filled glovebox, prior to use in catalysis, to rule out the inclusion of moisture when adding the base.

When using a coarse grain size of  $\text{Na}_2\text{CO}_3$ , 59% acetoin is obtained at a selectivity of 81% (entry 2.1), whereas the same experiments with the as-obtained  $\text{Na}_2\text{CO}_3$  (entry 1.3) yield 73% acetoin. This delivers proof-of-concept that the activation of the **IM-NHC5** catalyst is hampered by a larger grain size of  $\text{Na}_2\text{CO}_3$ . The finding in entry 2.2 further supports the assumption that the available base surface has a crucial role in the activation of the pre-catalyst. As the particle size is decreased, consequently, more exposed accessible surface becomes available, yielding 78% acetoin at an exceptional selectivity of 93%. Further decreasing the particle size with the sieve fraction  $\leq 200$   $\mu\text{m}$  results in an improved yield of 85% acetoin at a selectivity of 96% with negligible amounts of side products (entry 2.3). Hence, more acetoin is produced when using finer grain sizes of base and thus larger amounts of exposed

**Table 2** Results of the **IM-NHC5**-catalysed acetaldehyde self-addition in EtOH as the solvent using different mesh fractions of solid  $\text{Na}_2\text{CO}_3$  as the base<sup>a</sup>



Entry	Sieve fraction <i>d</i> ( $\mu\text{m}$ )	Y (acetoin) <sup>b,c</sup> (%)	$\sum Y$ (side products) <sup>b,d</sup> (%)	S (acetoin) (%)
2.1	$\geq 300$	59	13	81
2.2	$200 < d < 300$	78	6	93
2.3	$\leq 200$	85	4	96

<sup>a</sup> Reaction conditions: experiments were carried out using a stock solution containing acetaldehyde, ethanol and mesitylene in a 1:1:0.1 volumetric ratio.  $V(\text{stock}) = 2.0$  mL,  $n(\text{acetaldehyde}) \approx 19$  mmol,  $c(\text{IM-NHC5}) = 2$  mol%,  $T = 70$  °C,  $t = 2$  h, 1000 rpm. <sup>b</sup> As determined by GC-FID using mesitylene as the internal standard. <sup>c</sup> Acetoin yields including the yield of dimeric acetoin. <sup>d</sup> Side products include 1,1-diethoxyethane, paraldehyde and others.

$\text{Na}_2\text{CO}_3$  surface, supporting the postulated relationship between the portion of the catalyst being active and the amount of solid base surface. Findings from Tables 1 and 2 indicate that sieve fractions  $\leq 200$   $\mu\text{m}$  at a base concentration of 5.2 mol% are optimal for the catalytic productivity of the system.

In order to understand the effect of the higher base concentration on the performance of the continuous flow setup as well as the effect of the additional base on the catalyst stability, an experiment was carried out using a continuous stirred-tank reactor (CSTR) setup.<sup>19</sup> The exact description and flow diagram of the CSTR setup can be found in the SI (Fig. S1). In Fig. 1, a simplified schematic representation of the CSTR setup is shown.

The CSTR setup consists of a cooled reservoir for storage of the acetaldehyde-containing substrate mixture, which is fed to the heated reactor *via* a pump. Characterization of the CSTR setup led to developing a relationship between the volumetric flow rate of the substrate mixture and the average residence time which was obtained (see sections 1.1 and 1.2 in the SI). The back-pressure-regulator (BPR) installed downstream of the reactor is used to adjust the pressure of the system and to prevent runaway of acetaldehyde at reaction temperatures. After the BPR, the product stream is passed to the collection vessel, where samples can be withdrawn and the product can be stored.

Initially, a base concentration of 2.6 mol% with a particle size  $\leq 200$   $\mu\text{m}$  was used in the first 300 min TOS to allow for a comparison with the performance of the system published earlier. Therefore, key catalytic performances of the **IM-NHC5**/ $\text{Na}_2\text{CO}_3$  catalysed system discussed in the literature have been listed in Fig. 2 as well.

The additional crushing of  $\text{Na}_2\text{CO}_3$  has a significant influence on the activity of the system during the first 300 min TOS (Fig. 2, region I). For this experiment, an induction period was obtained, *i.e.*, it took a longer TOS before the product emerged from the reactor. Additionally, a maximum conversion/yield of 57% was attained after 225 min TOS. For the system using as-obtained  $\text{Na}_2\text{CO}_3$ , a maximum conversion/yield of 42% was observed after 135 min TOS (Fig. 2B). In Fig. 2A, about 45% of catalytically active centres are lost, based on the leaching values obtained from XRF after 300 min TOS. This loss in catalytic active centres is somewhat more compared to a similar

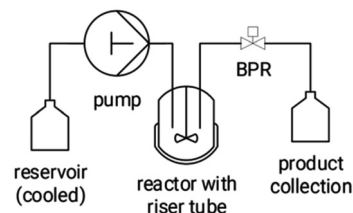


**Fig. 1** Schematic representation of the continuous stirred-tank (CSTR) reactor setup used for the continuous-flow acetaldehyde self-addition to acetoin. A more elaborate description of the reactor can be found in the SI of this manuscript (Fig. S1).



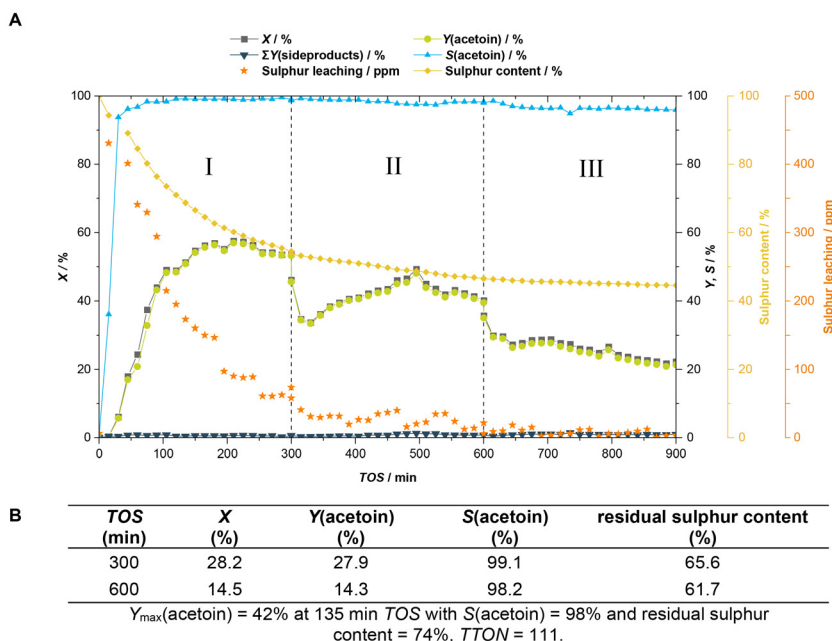


**Fig. 2** (A) Results of the continuous flow acetaldehyde self-addition in a CSTR setup over a total of 15 h TOS with intermittent  $\text{Na}_2\text{CO}_3$  addition after 300 min TOS (2 cycles). The graph shows the conversion  $X$ , yield  $Y$  and selectivity  $S$  towards acetoin over TOS as well as the calculated residual sulphur content (%) of the catalyst and the measured leaching of  $S$  (ppm) for samples taken every 15 minutes for a duration of 4 minutes. Dotted vertical lines at 300 and 600 min TOS indicate that the reaction was terminated overnight and restarted the next day after adding fresh  $\text{Na}_2\text{CO}_3$ . Reaction conditions: stock solution containing acetaldehyde (350 mL, 274.8 g, 6.2 mol), EtOH (350 mL, 275.3 g, 6.0 mol) and mesitylene (40.0 mL, 33.94 g),  $V(\text{stock}) = 0.475 \text{ mL min}^{-1}$ ,  $m(\text{IM-NHC5}) = 1.7403 \text{ g}$  ( $3.24 \text{ mmol g}^{-1}$ ,  $5.64 \text{ mmol NHC}$ ,  $2 \text{ mol}\%$ ),  $m(\text{Na}_2\text{CO}_3) = 779.6 \text{ mg}$  ( $7.36 \text{ mmol}$ ,  $2.6 \text{ mol}\%$ ),  $T = 70 \text{ }^\circ\text{C}$ ,  $1000 \text{ rpm}$ . (B) Tabular representation of the relevant catalytic results obtained from a comparable system described in the literature.<sup>19</sup>

CSTR experiment shown in previous work, where 38% was lost during the first 300 min TOS (compare Fig. 2A region I with Fig. 2B). The first 300 min TOS (Fig. 2, region I) highlight the role of the base in the overall productivity of the system, particularly when the performances of the sieved  $\text{Na}_2\text{CO}_3$ -based system discussed here are compared with that of the system using as-obtained  $\text{Na}_2\text{CO}_3$  shown in Fig. 2B. To facilitate a base concentration of 5.2 mol%, the reaction was terminated after 300 min TOS and the reactor was quickly cooled to room temperature and left to stand overnight. The next day (beginning of region II), upon the addition of an additional 2.6 mol% of  $\text{Na}_2\text{CO}_3$  to the reactor, the catalytic activity is partially restored between 300 and 500 min TOS and reaches a maximum value of 48% after a total of 495 min TOS (Fig. 2, region II), before conversions and yields drop to about 40% after 600 min TOS. As far as the leaching is concerned, the addition of another 1.3 eq. of base at 300 min TOS does not influence the leaching trend observed during the first 300 min TOS. Similarly, selectivity towards acetoin is not affected by the addition of base to the system. Selectivity values of >96% are observed throughout region II. The addition of another 1.3 eq. of  $\text{Na}_2\text{CO}_3$  and thus elevating the concentration of base to 5.2 mol% seems to be beneficial for the productivity of the catalyst. This observation was also hinted at from batch experiments (Table 1). At the same time, the extra addition of base does not have a suppressing effect on the catalyst decompo-

sition. The trends in sulphur leaching continued throughout region II. After the second base addition at 600 min TOS (Fig. 2, beginning of region III), another moderate increase in catalytic activity is observed from the yield-over-time curve. The activity of the system declines faster in region III after 750 min compared to the decline observed in region II. A minor decline in overall selectivity of the system is also observed. It is assumed that this is caused by the decay in catalytic activity of the NHC catalyst as well as the rather large amount of base present in the system. This could have led to the blocking of the catalytically active centres and consequently resulted in the observed lower productivity. More aldol side products are observed in region III compared to regions I and II. For all three regions, residual catalytic activity is still >20% at an excellent selectivity. For this CSTR experiment, a space-time-yield of  $56 \text{ g L}^{-1} \text{ h}^{-1}$  and a  $TTON = 230$  were obtained. These values resemble a clear improvement over the system previously reported in the literature, where no intermittent addition of  $\text{Na}_2\text{CO}_3$  was performed (Fig. 2B).<sup>19</sup> In both this work and previous work by our group, the TON and TTON are nominal values and do not take into account the leaching of the catalyst.

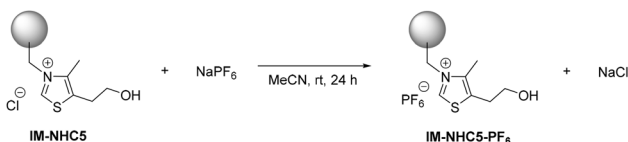
#### Structural modification of the IM-NHC5 catalyst

Despite the fact that the intermittent addition of  $\text{Na}_2\text{CO}_3$  resulted in a more productive IM-NHC5 catalytic system, an



enhancing effect with regard to catalyst stability could not be observed. In order to suppress this decomposition reaction, we prepared a structurally modified **IM-NHC5-PF<sub>6</sub>** catalyst, bearing a non-nucleophilic PF<sub>6</sub><sup>-</sup> counterion instead of a nucleophilic Cl<sup>-</sup> anion. Starting from pristine **IM-NHC5**, an ion exchange procedure was carried out, as commonly described in the literature for halide-based ionic liquids (Scheme 2).<sup>23–25</sup>

Based on post-modification elemental analysis, the loading of the catalytically active component on the PF<sub>6</sub><sup>-</sup>-modified catalyst was calculated to be 2.27 mmol g<sup>-1</sup>, whereas that of the unmodified **IM-NHC5** used in this experiment was calculated to be 2.87 mmol g<sup>-1</sup>. During the ion exchange procedure, some 4-methyl-5-thiazole ethanol is washed off due to the reverse Menshutkin reaction, indicating that the reaction itself is ongoing at all times and that catalyst decomposition is most probably not a consequence of the catalytic reaction. In order to still achieve comparable results with the **IM-NHC5** and its PF<sub>6</sub><sup>-</sup>-modified analog, the total amount of catalytically active component has to be kept constant, resulting in a greater mass of **IM-NHC5-PF<sub>6</sub>**. Strikingly, after the ion exchange procedure, the PF<sub>6</sub><sup>-</sup> loading in **IM-NHC5-PF<sub>6</sub>** was found to be 2.27 mmol g<sup>-1</sup> as well, highlighting that each Cl<sup>-</sup> anion of each catalytically active centre is replaced with a non-nucleophilic PF<sub>6</sub><sup>-</sup> counterion. With the modified catalyst in hand, we carried out several batch experiments where **IM-NHC5-PF<sub>6</sub>** was



**Scheme 2** Ion exchange of **IM-NHC5** with sodium hexafluorophosphate in acetonitrile to afford the PF<sub>6</sub> derivatised **IM-NHC5-PF<sub>6</sub>**.

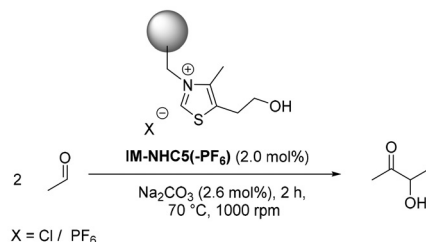
benchmarked against the performance of the unmodified, pristine **IM-NHC5** catalyst reported recently (Table 3).<sup>19</sup>

The successful formation of the **IM-NHC5-PF<sub>6</sub>** catalyst was shown by solid-state NMR spectroscopy. <sup>13</sup>C and <sup>31</sup>P solid-state NMR experiments were performed on **IM-NHC5-PF<sub>6</sub>** as shown in Fig. 3. The <sup>1</sup>H-<sup>13</sup>C cross-polarization (CP) spectrum resembles the one reported previously for **IM-NHC5** with chlorine as the counterion.<sup>19</sup> The <sup>1</sup>H-<sup>31</sup>P CP spectrum reveals the expected septet line shape for the PF<sub>6</sub><sup>-</sup> counter ion. The fact that the anion can be observed in such a CP spectrum indicates its successful immobilization.

Comparing the single run catalytic performance of the modified **IM-NHC5-PF<sub>6</sub>** catalyst (entry 3.1) with that of the pristine **IM-NHC5**, it can be observed that both catalysts give roughly similar results with respect to yield, selectivity and TON. Comparing the leaching of sulphur, as obtained from XRF measurements, reveals that much less sulphur is leached into the reaction solution for the **IM-NHC5-PF<sub>6</sub>** catalyst. After a typical reaction, about 21 ppm of sulphur is found to be present in the post-reaction solution of the **IM-NHC5-PF<sub>6</sub>** catalyst, whereas in the post-reaction solution of **IM-NHC5**, almost triple the amount of sulphur is found to be present in the post-reaction solution (58 ppm, entry 3.2). Regarding the amount of leached sulphur as an indicator of catalyst stability, the results obtained with **IM-NHC5-PF<sub>6</sub>** are much more promising for further investigating both batch and continuous flow applications. In Fig. 4, the results of ten consecutive batch recycling experiments are visualised.

Experiments were carried out using the same procedure reported earlier for the developed **IM-NHC5/Na<sub>2</sub>CO<sub>3</sub>** catalytic system. Again, after each run, the post-reaction solution was retrieved whilst ensuring that the catalyst beads stayed in the reactor before adding a new substrate to the reactor vessel.<sup>19</sup> In the first catalytic run, around 75% acetoin was observed. In the second catalytic run, a small decrease in catalytic activity was apparent, reflected by a yield of 66% acetoin. For runs

**Table 3** Catalytic results of two batch experiments carried out with **IM-NHC5-PF<sub>6</sub>/Na<sub>2</sub>CO<sub>3</sub>** as well as the results of a comparable experiment carried out with unmodified **IM-NHC5**<sup>a</sup>



Entry	Catalyst	Y (acetoin) <sup>b</sup> (%)	∑Y (side products) <sup>c</sup> (%)	TON (acetoin)	Sulphur <sup>d</sup> leaching (ppm)
3.1	<b>IM-NHC5-PF<sub>6</sub></b>	75	1.9	37	21
3.2 <sup>e</sup>	<b>IM-NHC5</b>	75	3.8	38	58

<sup>a</sup> Reaction conditions: *V*(acetaldehyde) = 1.0 mL, *n*(acetaldehyde) = 17.8 mmol, *V*(EtOH) = 1.0 mL, *c*(cat.) = 2 mol%, *c*(base) = 2.6 mol%, *T* = 70 °C, *t* = 2 h, 1000 rpm. <sup>b</sup> As determined by GC-FID using mesitylene as the internal standard. <sup>c</sup> Side products include 1,1-diethoxyethane, paraldehyde and others. <sup>d</sup> As determined *via* XRF measurements of the filtered post-reaction solution. <sup>e</sup> Result as described in ref. 19.



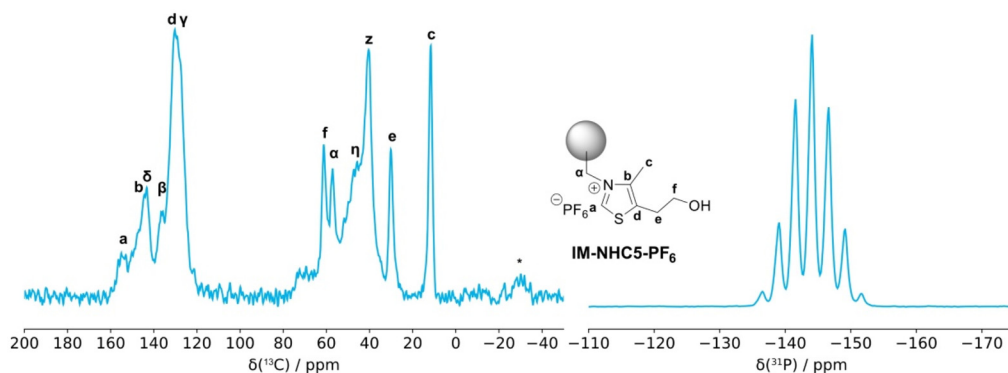


**Fig. 3**  $^1\text{H}$ - $^{13}\text{C}$  (left) and  $^1\text{H}$ - $^{31}\text{P}$  (right, with a zoomed-in view) CP spectra of **IM-NHC5-PF<sub>6</sub>** recorded at 14.0 kHz magic-angle spinning at a static magnetic field strength of 16.4 T. For the numbering of the resonances in the left spectrum, see the chemical structure; signals  $\beta$ ,  $\gamma$ ,  $\delta$  and  $\eta$  correspond to the polymeric support. A more detailed assignment can be found in ref. 19. \* indicates MAS sidebands.

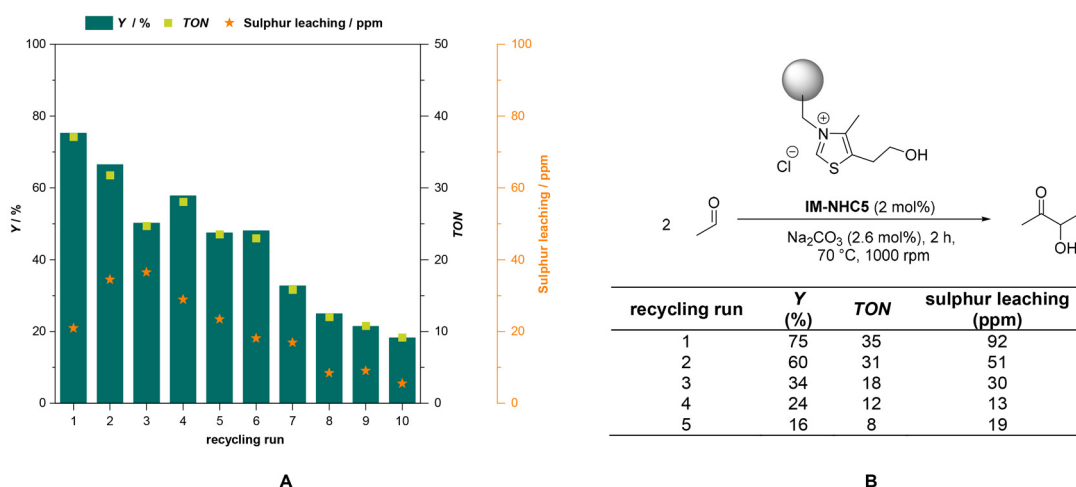


**Fig. 4** (A) Graphical representation of the results obtained from ten consecutive recycling runs using the **IM-NHC5-PF<sub>6</sub>**/ $\text{Na}_2\text{CO}_3$  catalyst system in the acetaldehyde self-addition to acetoin. (B) A tabular representation of the results obtained using the pristine **IM-NHC5**/ $\text{Na}_2\text{CO}_3$  system reported in the literature.<sup>19</sup> Reaction conditions:  $m(\text{IM-NHC5-PF}_6) = 156.2$  mg (0.4 mmol, 2.0 mol%),  $m(\text{Na}_2\text{CO}_3) = 53.6$  mg (0.5 mmol, 2.6 mol%),  $T = 70$  °C,  $t = 2$  h, 1000 rpm; yields determined by GC-FID using mesitylene as the internal standard.

three to six, acetoin yields remain relatively constant around 50% with a small outlier of 57% in run four. After the sixth run, the catalytic activity decreases seemingly faster compared to the previous runs. Still, after ten consecutive batch recycling experiments with a total reaction time of 20 h TOS, 20% acetoin is attained in the post-reaction solution. A TTON of 216 is obtained over the course of ten batch experiments. For the unmodified **IM-NHC5**, only five consecutive runs were carried out due to extensive catalyst decomposition. The  $\text{PF}_6$ -modified catalyst still exhibits very high activity after five runs (around 60% acetoin yield). For the unmodified **IM-NHC5**/ $\text{Na}_2\text{CO}_3$  system, only 16% acetoin was attained after five runs.<sup>19</sup> Also, much lower leaching values of sulphur are attained for the **IM-NHC5-PF<sub>6</sub>** system compared to the unmodified **IM-NHC5** system.<sup>19</sup> These results are very promising and support the assumption that the **IM-NHC5-PF<sub>6</sub>** catalyst has an increased stability and a decreased tendency to

undergo decomposition. As the leaching of sulphur was found to be lower from XRF measurements, we also investigated the spent catalyst using solid-state NMR spectroscopy to see if there is spectroscopic evidence for the presence of catalytically active species, *i.e.*, free carbenes, even after 10 consecutive batch experiments.

The  $^1\text{H}$ - $^{13}\text{C}$  CP-MAS spectrum of the spent catalyst reveals several spectral changes with respect to the initial spectrum of **IM-NHC5-PF<sub>6</sub>** (Fig. 3) such as the appearance of additional resonances between 80 and 120 ppm, which indicate currently unexplained structural or electronic changes in the catalyst during the reaction (Fig. S6). In addition, the resonance at the highest  $^{13}\text{C}$  chemical-shift values ( $\sim 160$  ppm) experiences further deshielding after the reaction. Dipolar dephasing CP-MAS (DD-CPMAS) experiments reveal that this resonance can be assigned to a quaternary carbon atom (Fig. S7), possibly resulting from the activated carbene species, which would



further support the high stability of the catalyst during the reaction as there still are activated carbene species left in the catalyst after 10 batch recycling experiments (Fig. 4A). However, stable carbene species are reported in the literature to exhibit a slightly higher shift of 200–250 ppm.<sup>26</sup>

Considering the presence of active carbene species after the recycling experiments, the **IM-NHC5-PF<sub>6</sub>** catalyst seems very promising for a long-term performance test in a closed continuous flow reactor (CSTR). In total, the catalyst was kept on stream for a total of somewhat over 60 h, and various reaction conditions were tested while keeping the catalyst in the loop to exploit its potential (Fig. 5).

During the first 6 h TOS, the obtained values for conversion and acetoin yield for the **IM-NHC5-PF<sub>6</sub>**/Na<sub>2</sub>CO<sub>3</sub> system are somewhat lower compared to the experiment carried out earlier (Fig. S3). Around 10% of conversion/yield is observed at a maximum selectivity of around 92%, dropping steadily to 85% after 6 h TOS. The observed effect and the apparent deviation from the trend can be explained by the lower stirring speed that was investigated in this region. The stirring speed was only set to 500 rpm in Fig. 5, region I, to evaluate the effect of stirring speed on the performance of the catalyst. The

fact that a lower-than-expected catalytic activity is observed highlights the necessity of highly dispersing the solid Na<sub>2</sub>CO<sub>3</sub> in order to activate the catalyst which is ensured by strong mixing (*i.e.*, higher rpm). Interestingly, during the first 6 h TOS, only 8% of the initial amount of catalytically active component (residual S content) is lost, whereas during earlier conducted CSTR experiments with the pristine **IM-NH5**/Na<sub>2</sub>CO<sub>3</sub> system described in the literature, almost 30% of the initial sulphur is leached into solution during the same reaction time of 6 h TOS.<sup>19</sup>

After 6 h TOS, the stirring speed was increased to 1000 rpm. Accordingly, this results in a better mixing inside the reactor, presumably an improved mass transfer, and consequently, conversion and yield levels rise throughout region II to 20% at a selectivity of  $S(\text{acetoin}) > 96\%$ . In regions III and IV, no intermittent changes to the reaction conditions were made. Both yields and conversions slowly drop to about 16%. Additionally, the selectivity towards acetoin drops to 91%. However, after about 24 h TOS (end of region IV), the modified **IM-NHC5-PF<sub>6</sub>** catalyst is still active and contains about 86% residual sulphur. The first regions I to IV already highlight that the PF<sub>6</sub>-modified catalyst is less prone to undergo the

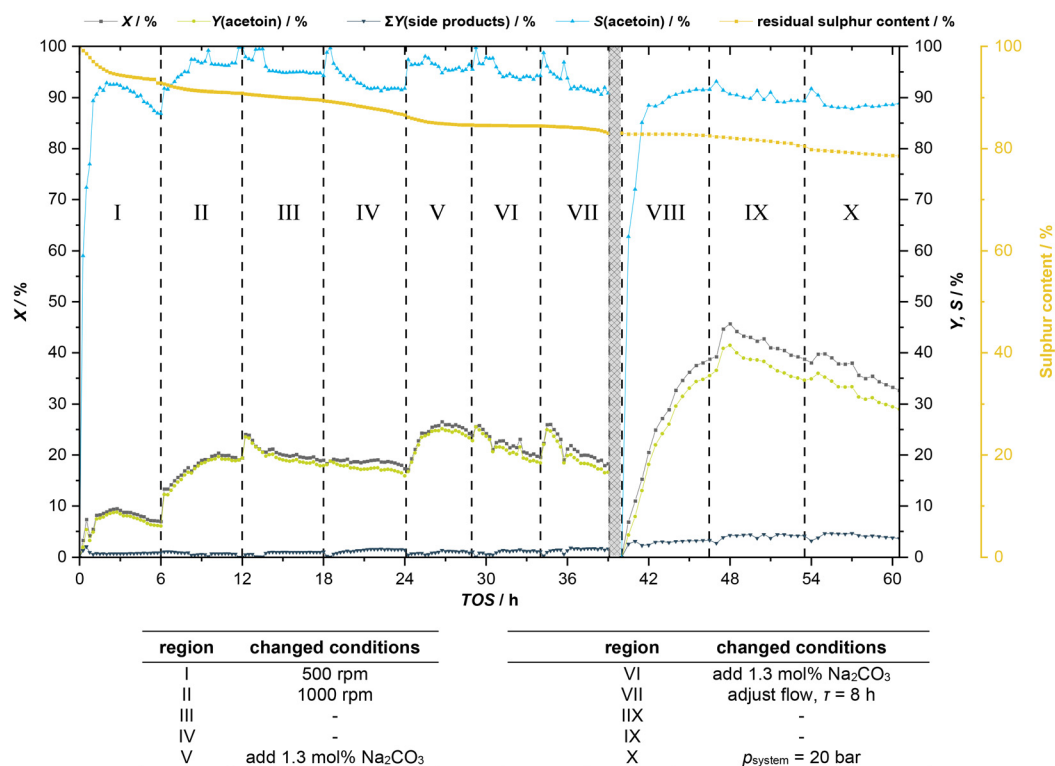


**Fig. 5** Results of the continuous-flow acetaldehyde self-addition in a CSTR setup over a total of 60 h TOS. The graph shows the conversion  $X$ , yield  $Y$  and selectivity  $S$  towards acetoin over TOS as well as the calculated residual sulphur content (%) of the catalyst. Reaction conditions: stock solution containing acetaldehyde EtOH and mesitylene,  $\dot{V}(\text{stock}) = 0.475 \text{ mL min}^{-1}$  for  $0 \text{ h} < \text{TOS} < 39 \text{ h}$ ,  $\dot{V}(\text{stock}) = 0.148 \text{ mL min}^{-1}$  for  $\text{TOS} > 39.5 \text{ h}$ ,  $m(\text{IM-NHC5-PF}_6) = 2.49 \text{ g}$  ( $2.27 \text{ mmol g}^{-1}$ ,  $5.65 \text{ mmol NHC}$ ,  $2 \text{ mol}\%$ ),  $m(\text{Na}_2\text{CO}_3) = 775.0 \text{ mg}$  ( $7.31 \text{ mmol}$ ,  $2.6 \text{ mol}\%$ ),  $T = 70 \text{ }^\circ\text{C}$ ,  $\tau = 2 \text{ h}$  for  $0 \text{ min} < \text{TOS} < 39 \text{ h}$ ,  $\tau = 8 \text{ h}$  for  $\text{TOS} > 39.5 \text{ h}$ ,  $1000 \text{ rpm}$ . Mass-balances  $\sum Y > 90\%$  were obtained. Dotted lines indicate that the reaction was terminated overnight and restarted the next day and/or changes were made with regard to the flow rate, *i.e.*, residence time of the substrate-containing stock solution. The grey masked area around 39 h indicates flushing of the reactor with EtOH at a flow rate of  $\dot{V}(\text{EtOH}) = 3.0 \text{ mL min}^{-1}$ . The measured leaching of S (ppm) has been omitted for clarity and can be found in the SI. On average, about 4 ppm of sulphur loss was observed in each sample.



reverse Menshutkin reaction. As far as the catalytic performance is concerned, the catalyst seems to have a lower activity in the CSTR reactor compared to its unmodified predecessor **IM-NHC5** as lower acetoin yields are obtained.

As mentioned previously, the experiments in regions I to IV were carried out using the earlier established catalyst-to-base-ratio of 1:1.3 to be comparable to the results for **IM-NHC5** shown in region I of Fig. 2. In order to evaluate the effect of intermittent base addition to the reactor, 1.3 eq. of solid  $\text{Na}_2\text{CO}_3$  was introduced into the system at the beginning of region V. Clearly, this addition of base, increasing the concentration of base from 2.6 mol% to 5.2 mol%—the earlier established optimal catalyst-to-base-ratio (entry 1.4, Table 1)—boosts the productivity of the system. Again, the effect of intermittent base addition on the catalyst leaching behaviour is rather insignificant. Thus, the observations made here when using the modified catalyst **IM-NHC5-PF<sub>6</sub>** correspond to those made for its unmodified predecessor **IM-NHC5**.

At the beginning of regions VI and VII, another 1.3 eq. of base is added (a comparable procedure to that shown in Fig. 2). The catalytic productivity seems to increase less in region VI compared to region VII, a phenomenon not observed in previous experiments with pristine **IM-NHC5** (Fig. 2). Nevertheless, a decrease in catalytic productivity is apparent over the entire period from around 27 h TOS (middle of region V) to the end of region VII. However, it has to be noted that the modified catalyst is still active after 39 h TOS and that about 20% conversion is achieved with an acetoin yield of 18% and a selectivity of 90% with a residual sulphur content of about 83%.

Between 39 h TOS and 39.5 h TOS, the system was flushed with EtOH at a high flow rate of  $3.0 \text{ mL min}^{-1}$ . Afterwards, the feed of the substrate was re-initiated at a much lower rate of  $0.148 \text{ mL min}^{-1}$  to achieve an average residence time of  $\tau = 8 \text{ h}$  instead of  $\tau = 2 \text{ h}$ . The relationship between the flow rate of substrate and the average residence time of substrates in the reactor is described in the SI. In region VIII, as well as at the beginning of region IX, conversions increase to attain a maximum of 46% after 48 h TOS (region IX, Fig. 5), while the catalyst still has around 80% residual sulphur content left. Clearly, the productivity of the system benefits from longer residence times. However, presumably due to the longer residence time of the acetaldehyde in the reactor, acetaldehyde is more likely to undergo side reactions, leading to a higher yield of side products observed for a TOS exceeding 39.5 h. After attaining a maximum yield of 41% after 48 h TOS, catalytic activity decays to around 35% by the end of region IX. In region X, the pressure of the system was raised from the conventional 7 to 20 bar. No effect of the increased system pressure is observed, as the existing trends in terms of activity and catalyst decomposition appear to continue. After almost 60 h TOS, the system is still able to attain 29% acetoin yield at 32% substrate conversion. For the whole 60 h TOS, a total turn-over number of TTON = 600 is attained. The fact that the catalyst is still able to show very high activity towards the end of more than 60 h TOS at a residual sulphur content of 78% once

more highlights the substantial improvement made to the stability of the catalyst by means of the ion-exchange procedure.

## Conclusion

Within this study, two possible pathways for achieving an improved and more productive version of the earlier reported **IM-NHC5** catalyst<sup>19</sup> were highlighted: the role of the solid (mild) base and a structural modification of the catalyst itself. The investigations regarding the influence of solid  $\text{Na}_2\text{CO}_3$  used gave rise to the assumption that the activation of **IM-NHC5** proceeds *via* a surface reaction. As the reaction is assumed to be a surface reaction, it benefits from the total available surface of  $\text{Na}_2\text{CO}_3$  indicated by the fact that smaller sieve fractions of  $\text{Na}_2\text{CO}_3$  result in a higher overall activity of the catalyst. Intermittent additions of the solid base into the reactor could increase the overall productivity of the system, presumably by activating a larger portion of the catalyst. However, an effect on the rate of catalyst decomposition *via* the reverse Menshutkin reaction was not observed. To tackle the catalyst decomposition, the idea was developed to suppress the reaction by exchanging the nucleophilic  $\text{Cl}^-$  ion for non-nucleophilic  $\text{PF}_6^-$  ions to suppress a reverse Menshutkin decomposition pathway. Already in batch recycling experiments, the  $\text{PF}_6^-$ -modified immobilised NHC catalyst (**IM-NHC5-PF<sub>6</sub>**) outperformed the earlier reported unmodified **IM-NHC5** catalyst, and the loss of the catalytically active component could be significantly reduced.<sup>19</sup> In post-catalytic solid-state dipolar dephasing CP-MAS analysis, a quaternary carbon was found to be present, which could possibly be the activated carbene, underlining the enhanced stability of the catalyst upon ion exchange. Continuous flow catalytic tests revealed that the catalyst was active for over 60 h time-on-stream, and in the long-term study carried out, several reaction parameters and their influence on the performance of the catalytic system were evaluated, resulting in a total turn-over-number of 600 at an average yield of 20%. Considering an average mass balance of 92% for the long-term experiment, an isolable acetoin yield of 117 g was estimated.

## Experimental section

EtOH, HPLC Gradient Rotisolv® (<0.1%  $\text{H}_2\text{O}$ ), was purchased from CarlRoth and used without further purification. MeCN (>99.5%, for synthesis) was purchased from CarlRoth and used without further purification. Anhydrous MeOH (methanol 99.8%, extra dry over molecular sieve, AcroSeal®) was purchased from Acros Organics. Anhydrous acetaldehyde (>99.99%) was purchased from Sigma. Mesitylene purchased from Sigma (98%) and used as an internal standard for GC-FID measurements was dried over  $\text{MgSO}_4$  (obtained from Sigma) prior to employing it in substrate-containing stock solutions. (Chloromethyl) polystyrene (Merrifield's peptide



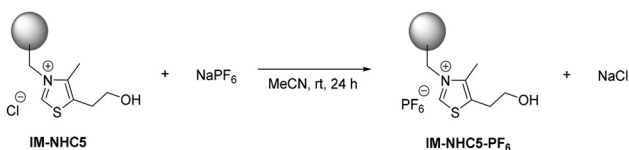
resin, porous, extent of labeling:  $\sim 5.5 \text{ mmol g}^{-1}$  Cl loading) and 4-methyl-5-thiazole ethanol (98%) were also obtained from Sigma. 4-Methyl-5-thiazole ethanol was degassed and stored over molecular sieves ( $4 \text{ \AA}$ ) prior to carrying out the grafting procedure. Sodium hexafluorophosphate used for the ion exchange procedure (98%) was purchased from Sigma and used without further purification.

Air-sensitive chemicals and catalysts were stored in an Ar-filled glovebox, and standard Schlenk techniques were applied.

GC-FID and GC-MS analyses were carried out on Shimadzu instruments using a Restek Rtx-1701 (30 m) column. ICP analysis was carried out by Mikroanalytisches Laboratorium Kolbe. XRF measurements were used to determine the sodium and sulphur content in post-reaction solutions. Measurements were carried out using a Spectro Xepos C instrument equipped with a Co-Pd-alloy X-ray source and a silicon-drift detector. Prior to carrying out a typical measurement, 1.0 mL of the filtered post-reaction sample was filled into a cuvette with an outer diameter of 20 mm and an inner diameter of 16 mm. The cuvette was covered with a  $12 \text{ \mu m}$  thick Prolene® foil. Measurements were carried out for 600 seconds in a mixed He/air atmosphere at an energy level of 3 keV to 19 keV. Recalibration of the device was carried out daily, using a glass tablet with a known elemental composition.<sup>19</sup>

$\text{Na}_2\text{CO}_3$  sieve fractions were prepared as follows: rather coarse  $\text{Na}_2\text{CO}_3$  (Sigma) was crushed by hand for at least 5 minutes, using a pestle and mortar. Afterwards, the crushed  $\text{Na}_2\text{CO}_3$  was loaded onto a column of two sieves (VWR, ISO 3310, NF ISO 3310, BS 410,  $200 \times 50 \text{ mm}$  – stainless steel frame AISI 304, stainless steel wire cloth AISI 316) where the upper sieve had a wire mesh of  $300 \text{ \mu m}$  and the bottom sieve a wire mesh of  $200 \text{ \mu m}$ . The sieve column was shaken manually. This setup allowed for the collection of  $\text{Na}_2\text{CO}_3$  sieve fractions with particle sizes  $d \geq 300 \text{ \mu m}$ ,  $200 < d < 300 \text{ \mu m}$  and  $d \leq 200 \text{ \mu m}$ . After collecting the sieve fractions, the samples were thoroughly dried in an oven set to  $120 \text{ }^\circ\text{C}$  for at least 24 h, prior to storing in an Ar-filled glovebox until used in catalytic experiments.

### Preparation of IM-NHC5-PF<sub>6</sub>



The ion exchange procedure was carried out using a batch of **IM-NHC5** prepared according to the procedures described in the literature.<sup>19</sup> **IM-NHC5** ( $7.8809 \text{ g}$ ,  $2.78 \text{ mmol g}^{-1}$ ,  $21.9 \text{ mmol}$ ,  $1.0 \text{ eq.}$ ) was suspended in MeCN ( $120 \text{ mL}$ ). To that was added  $\text{NaPF}_6$  ( $6.655 \text{ g}$ ,  $39.6 \text{ mmol}$ ,  $1.8 \text{ eq.}$ ) in Ar counterflow. The ion exchange reaction was carried out for 24 h at room temperature using a low stirring speed of  $100 \text{ rpm}$  to avoid abrasion of the **IM-NHC5** catalyst beads. Afterwards, a white precipitate was observed. Volatiles were removed *in vacuo*, and  $\text{H}_2\text{O}$  ( $40 \text{ mL}$ ) was added to extract NaCl and unconverted  $\text{NaPF}_6$ . The brine was removed *via* cannula filtration

under Ar counterflow, and the obtained beads were washed with anhydrous MeOH ( $4 \times 10 \text{ mL}$ ). After washing, the pre-catalyst beads were dried *in vacuo* and stored in an Ar-filled glovebox for further use. The loading of the catalyst was calculated to be  $2.27 \text{ mmol g}^{-1}$ , based on the results of the elemental analysis of the catalyst (Mikroanalytisches Labor Kolbe). The amount of  $\text{PF}_6$  was found to be  $2.27 \text{ mmol g}^{-1}$  as well, indicating complete ion exchange of the grafted catalyst.

### General procedure for (batch recycling) experiments using the IM-NHC5/IM-NHC5-PF<sub>6</sub> pre-catalyst and base

In the case of batch experiments, inside an Ar-filled glovebox, either the pre-catalyst **IM-NHC5** or the modified **IM-NHC5-PF<sub>6</sub>** as well as  $\text{Na}_2\text{CO}_3$  was added to a thick-walled glass pressure tube (ACE,  $20 \text{ mL}$ ). Outside the glovebox, either an acetaldehyde and mesitylene containing stock solution in ethanol or acetaldehyde, ethanol, and mesitylene separately was added. In both cases, the addition of substrate and solvent was carried out under Ar counterflow. The pressure tube was tightly closed, heated in an oil bath at the indicated temperature and stirred for the indicated time. Afterwards, the mixture was allowed to reach room temperature before submerging in an ice bath for 15 minutes. The liquid contents of the pressure tube were retrieved *via* cannula filtration and subjected to GC-FID analysis. Response factors for acetoin and acetaldehyde were determined by calibration using mesitylene as an internal standard. The procedures for a typical continuous flow reaction, as well as the description of the continuous flow reactor itself, can be found in the literature.<sup>19</sup>

### Solid-state NMR

The solid-state NMR spectra were recorded at magnetic-field strengths of  $11.7$  and  $16.4 \text{ T}$  using Bruker double- and triple-resonance  $3.2 \text{ mm}$  probes. The spectra were processed with the software ssNake (version 1.5) using Gaussian apodization of  $100 \text{ Hz}$  as defined in the software.<sup>27</sup> The experimental  $^1\text{H}$ - $^{13}\text{C}$  and  $^1\text{H}$ - $^{31}\text{P}$  CP conditions were optimized directly on the samples where possible, or using  $^{13}\text{C}$  solid adamantane in samples with low signal-to-noise ratios in the corresponding spectra.  $^{13}\text{C}$  spectra were referenced to TMS using the methylene resonance of adamantane as an external standard.<sup>28</sup>  $^{31}\text{P}$  spectra were referenced to  $85\% \text{ H}_3\text{PO}_4$  using the *O*-phospho-L-serine resonance as an external standard.<sup>29</sup> The spectra were recorded at a probe temperature of  $293 \text{ K}$ . For the experimental details, see the SI.

### Conflicts of interest

The authors have no conflicts of interest to declare.

### Data availability

The data supporting this article have been included as part of the supplementary information (SI). Supplementary information is available. See DOI: <https://doi.org/10.1039/d5gc03630e>.



## Acknowledgements

The Max Planck Society is acknowledged for funding. M. B. acknowledges the networking programme 'Sustainable Chemical Synthesis 2.0' for support and discussions across disciplines. The authors thank A. Jakubowski, A. Gurowski and J. Werkmeister for analytical support. T.W. appreciates the funding by the Deutsche Forschungsgemeinschaft (DFG, German Research Foundation) under Germany's Excellence Strategy – Exzellenzcluster 2186 "The Fuel Science Center" (ID: 390919832) and acknowledges further support from the DFG (Heisenberg fellowship, project number 455238107). Open Access funding was provided by the Max Planck Society.

## References

- N. M. Eagan, M. D. Kumbhalkar, J. S. Buchanan, J. A. Dumesic and G. W. Huber, *Nat. Rev. Chem.*, 2019, **3**, 223–249.
- J. M. Restrepo-Flórez and C. T. Maravelias, *Energy Environ. Sci.*, 2021, **14**, 493–506.
- R. A. Dagle, A. D. Winkelman, K. K. Ramasamy, V. L. Dagle and R. S. Weber, *Ind. Eng. Chem. Res.*, 2020, **59**, 4843–4853.
- K. S. Rawat, S. C. Mandal, P. Bhauriyal, P. Garg and B. Pathak, *Catal. Sci. Technol.*, 2019, **9**, 2794–2805.
- M. C. Xue, B. L. Yang, C. G. Xia and G. L. Zhu, *ACS Sustainable Chem. Eng.*, 2022, **10**, 3466–3476.
- S. Chakraborty, P. E. Piszal, C. E. Hayes, R. T. Baker and W. D. Jones, *J. Am. Chem. Soc.*, 2015, **137**, 14264–14267.
- K. N. Tseng, S. Lin, J. W. Kampf and N. K. Szymczak, *Chem. Commun.*, 2016, **52**, 2901–2904.
- I. Nezam, J. Zak and D. J. Miller, *Ind. Eng. Chem. Res.*, 2020, **59**, 13906–13915.
- A. Galadima and O. Muraza, *Ind. Eng. Chem. Res.*, 2015, **54**, 7181–7194.
- A. Ohligschläger, N. van Staaldunen, C. Cormann, J. Mühlhans, J. Wurm and M. A. Liauw, *Chem.: Methods*, 2021, **1**, 181–191.
- G. Pomalaza, P. Arango Ponton, M. Capron and F. Dumeignil, *Catal. Sci. Technol.*, 2020, **10**, 4860–4911.
- E. V. Makshina, M. Dusselier, W. Janssens, J. Degreve, P. A. Jacobs and B. F. Sels, *Chem. Soc. Rev.*, 2014, **43**, 7917–7953.
- L. Clarizia, R. Andreozzi, J. Apuzzo, I. Di Somma and R. Marotta, *Chem. Eng. J.*, 2020, **393**, 123425.
- J. Rehbein, S. M. Ruser and J. Phan, *Chem. Sci.*, 2015, **6**, 6013–6018.
- R. Breslow, *J. Am. Chem. Soc.*, 1958, **80**, 3719.
- D. Enders, O. Niemeier and A. Henseler, *Chem. Rev.*, 2007, **107**, 5606–5655.
- L. Gu, T. Lu, X. Li and Y. Zhang, *Chem. Commun.*, 2014, **50**, 12308–12310.
- T. Lu, X. Li, L. Gu and Y. Zhang, *ChemSusChem*, 2014, **7**, 2423–2426.
- M. Belleflamme, J. Hommes, R. Dervisoglu, E. Bartalucci, T. Wiegand, A. K. Beine, W. Leitner and A. J. Vorholt, *ChemSusChem*, 2024, **17**, e202400647.
- W. Awad, J. Gilman, M. Nyden, R. Harris Jr and T. Sutto, *Thermochim. Acta*, 2004, **409**, 3.
- H. Ohtani, S. Ishimura and M. Kumai, *Anal. Sci.*, 2008, **24**, 1335–1340.
- E. Deruer, N. Duguet and M. Lemaire, *ChemSusChem*, 2015, **8**, 2481–2486.
- N. D. Vu, S. Bah, E. Deruer, N. Duguet and M. Lemaire, *Chem. – Eur. J.*, 2018, **24**, 8141–8150.
- I. Dinarès, C. Garcia de Miguel, A. Ibáñez, N. Mesquida and E. Alcalde, *Green Chem.*, 2009, **11**, 1507–1510.
- E. Alcalde, I. Dinares, A. Ibanez and N. Mesquida, *Molecules*, 2012, **17**, 4007–4027.
- D. Bourissou, O. Guerret, F. P. Gabbaï and G. Bertrand, *Chem. Rev.*, 2000, **100**, 39–92.
- S. G. J. van Meerten, W. M. J. Franssen and A. P. M. Kentgens, *J. Magn. Reson.*, 2019, **301**, 56–66.
- C. R. Morcombe and K. W. Zilm, *J. Magn. Reson.*, 2003, **162**, 479–486.
- R. K. Harris, E. D. Becker, S. M. Cabral de Menezes, R. Goodfellow and P. Granger, *Pure Appl. Chem.*, 2001, **73**, 1795–1818.

